

Geometric Bounds on the Power of Adiabatic Thermal Machines

Joshua Eglinton and Kay Brandner

*School of Physics and Astronomy, University of Nottingham, Nottingham NG7 2RD, United Kingdom
Centre for the Mathematics and Theoretical Physics of Quantum Non-equilibrium Systems,
University of Nottingham, Nottingham NG7 2RD, United Kingdom*

(Dated: February 18, 2022)

We analyze the performance of slowly driven meso- and micro-scale refrigerators and heat engines that operate between two thermal baths with small temperature difference. Using a general scaling argument, we show that such devices can work arbitrarily close to their Carnot limit only if heat-leaks between the baths are fully suppressed. Their power output is then subject to a universal geometric bound that decays quadratically to zero at the Carnot limit. This bound can be asymptotically saturated in the quasi-static limit if the driving protocols are suitably optimized and the temperature difference between the baths goes to zero with the driving frequency. These results hold under generic conditions for any thermodynamically consistent dynamics admitting a well-defined adiabatic-response regime and a generalized Onsager symmetry. For illustration, we work out models of a qubit-refrigerator and a coherent charge pump operating as a cooling device.

Dimensionless figures of merit, such as the efficiency of a heat engine or the coefficient of performance (COP) of a refrigerator, provide convenient measures for the performance of thermal machines. These figures are subject to universal bounds, which follow directly from the first and the second law of thermodynamics and are known as Carnot bounds [1]. To attain its Carnot bound, a thermal machine has to work without producing any net entropy. This condition is generally assumed to be met only if the machine does not exchange any heat with its environment or if it operates infinitely slow. In both cases the generated output per time is zero. Hence, the Carnot limit can be reached only at the price of vanishing power.

The question how this trade-off can be formulated quantitatively for meso- and micro-scale thermal machines, and whether it can be overcome in special situations, has attracted significant interest over the last decade [2–12]. As a result, a variety of trade-off relations that bound the power of different types of machines in terms of a dimensionless figure of merit were discovered, first in linear-response [13–17] and then far from equilibrium [18–27]. Since such bounds must go beyond the first and the second law, which due to the lack of a fundamental time scale do not provide any constraint on power, they have to be derived from the underlying dynamics of the system. As a result, different bounds hold for Markov jump processes [18–21], underdamped Fokker-Planck dynamics [18], Lindblad dynamics [22, 23] or coherent transport [24–26].

For adiabatic thermal machines, which use a working system that is driven by slow periodic variations of external control parameters, thermodynamic geometry provides a promising avenue towards a unified picture. This framework was originally developed for macroscopic systems [28–31] and later extended to classical meso- and micro-scale systems [32–35] as well as the quantum regime [36–38]. The key idea is that the time dependent state variables of the working system, e.g. the entries of

a density matrix, which in general have to be found by solving a non-autonomous set of differential equations, become functions of the control variables and their time derivatives if the driving is slow on some characteristic time scale of the system. Quantities like work or entropy production, which depend on these state variables, can thus be related to geometric objects such as vector fields or metrics in the space of control parameters. Once the dynamics of the system has been specified, the coefficients defining these objects can be calculated by means of adiabatic perturbation theory [39–41]. Any relation between the quantities of interest, however, that follows from general symmetries or purely geometric arguments, holds universally for any kind of thermodynamically consistent dynamics.

The geometric approach has led to notable insights on the principles that govern the performance of adiabatic thermal machines [42–50]. Recent results include explicit optimization schemes for different types of devices [51–56] as well as geometric trade-off relations between the efficiency, power yield [45] and power fluctuations [47] of cyclic heat engines that are driven by continuous temperature variations. These trade-off relations show that, close to the Carnot limit, the power of such devices is bounded by a linear function of their efficiency, which goes to zero at the Carnot value.

In this article, we consider a complementary setting, where an adiabatic machine works between two thermal baths with fixed temperatures. The thermodynamic geometry of this setup, which covers both heat engines and refrigerators, is usually developed by treating the temperature difference between the reservoir and the environment as a first-order perturbation along with the driving rates [51]. Here, we argue that this approach is no longer sufficient if the machine operates close to the Carnot limit. Specifically, we show that, in this regime, the performance of a generic machine is governed by second-order corrections in the temperature difference between

the baths. This effect leads to a new family of geometric trade-off relations implying a quadratic rather than a linear decay of power at the Carnot bound.

This behavior can be derived from a general scaling argument. To this end, it is convenient to introduce generalized fluxes J_x and affinities A_x such that the average rate of entropy production can be expressed in the standard form $\sigma = J_x A_x$, where summation over identical indices is understood throughout [57]. The fluxes J_x correspond to output and input of the machine and the affinities A_x represent the thermodynamic forces that drive the system away from equilibrium. For an adiabatic response theory, natural choices of these variables are

$$J_w = W, \quad J_q = Q/\tau, \quad A_w = \beta_e/\tau \quad \text{and} \quad A_q = \beta_e - \beta_r. \quad (1)$$

Here, τ denotes the cycle time, β_e and β_r are the inverse temperatures of the two baths, to which we refer as environment and reservoir; W and Q are the applied work and the heat uptake from the reservoir per operation cycle. Boltzmann's constant is set to 1 throughout.

We now focus on refrigerators. That is, we assume that $\beta_r \geq \beta_e$ and $W, Q \geq 0$ so that the machine absorbs work from the external driving and extracts heat from the cold reservoir. The performance of such a device is described by the COP $\varepsilon \equiv Q/W$, which is bounded by the Carnot value $\varepsilon_C \equiv \beta_e/(\beta_r - \beta_e)$. To determine under what conditions ε approaches ε_C , we divide the work input into an isothermal part and a correction stemming from the temperature difference between the reservoirs,

$$J_w^{\text{iso}} \equiv J_w|_{A_q=0} \equiv K_{ww}A_w \quad \text{and} \quad J_w - J_w^{\text{iso}} \equiv K_{wq}A_q. \quad (2)$$

Analogously, the heat flux can be divided into a quasi-static contribution and a finite-rate correction,

$$J_q^{\text{qs}} \equiv J_q|_{A_w=0} \equiv K_{qq}A_q \quad \text{and} \quad J_q - J_q^{\text{qs}} \equiv K_{qw}A_w. \quad (3)$$

The coefficients K_{xy} are functions of the affinities, which in general assume finite values in the limit $A_x \rightarrow 0$. Furthermore, the second law requires that $K_{ww}, K_{qq} \geq 0$ and time-reversal symmetry implies that the cross-coefficients obey the Onsager symmetry

$$K_{qw}|_{A_x=0} = -K_{wq}|_{A_x=0} \quad (4)$$

in zeroth order with respect to the affinities. This symmetry holds for arbitrary driving protocols as long as the system is not subject to external magnetic fields breaking time reversal symmetry, which we assume here.

The normalized COP can now be written in the form

$$\frac{\varepsilon}{\varepsilon_C} = -\frac{J_q A_q}{J_w A_w} = -\frac{K_{qw} + K_{qq}(A_q/A_w)}{K_{wq} + K_{ww}(A_w/A_q)}. \quad (5)$$

Since the isothermal work will in general not vanish, it is natural to assume that $K_{ww} > 0$. Owing to the Onsager symmetry (4), the expression (5) then converges to 1 in

the quasi-static limit $A_w \rightarrow 0$ if $K_{qq} = 0$ and $A_q \propto A_w^\alpha$ with $0 < \alpha < 1$. That is, provided that the quasi-static heat flux vanishes, the Carnot bound is attained asymptotically as both affinities go to zero with A_w vanishing faster than A_q , whereby both ε and ε_C diverge.

To determine how the cooling power J_q decays in this limit, we expand the coefficients K_{qw} and K_{wq} in the affinities keeping leading and first sub-leading terms,

$$K_{qw} = L_{qw} + L_{qw}^q A_q, \quad K_{wq} = -L_{qw} + L_{wq}^q A_q. \quad (6)$$

Inserting these expansions into Eq. (5) and again keeping only leading and first subleading terms leaves us with

$$\frac{\varepsilon}{\varepsilon_C} = 1 + \frac{L_{qw}^q + L_{wq}^q}{L_{qw}} A_q + \frac{L_{ww}}{L_{qw}} \frac{A_w}{A_q}, \quad (7)$$

where $L_{ww} \equiv K_{ww}|_{A_x=0}$. Upon maximizing the right-hand side of this equation with respect to A_q , we obtain an upper bound on $\varepsilon/\varepsilon_C$ and an optimum for the thermal gradient, which are given by

$$\varepsilon/\varepsilon_C \leq 1 - \sqrt{L_{qw} A_w / Z} \quad \text{and} \quad A_q^* = -\sqrt{z A_w} \quad (8)$$

with $Z \equiv L_{qw}^3 / 4(L_{wq}^q + L_{qw}^q) L_{ww}$ and $z \equiv L_{ww} / (L_{wq}^q + L_{qw}^q)$ being non-negative quantities [58]. Since $J_q = L_{qw} A_w$ in leading order, we can now replace A_w with J_q / L_{qw} in Eq. (8), which yields the power-COP trade-off relation

$$J_q \leq Z(\varepsilon_C - \varepsilon)^2 / \varepsilon_C^2. \quad (9)$$

This relation, which is our first main result, shows that the cooling power of a generic adiabatic refrigerator decays at least quadratically at the Carnot bound.

A similar picture emerges for adiabatic heat engines, which are realized for $\beta_r \leq \beta_e$, $Q \geq 0$ and $W \leq 0$. Hence, the machine picks up heat from the hot reservoir and generates work output. Its efficiency is then defined as $\eta \equiv -W/Q$ and the corresponding Carnot bound reads $\eta_C \equiv (\beta_e - \beta_r)/\beta_e$. Upon introducing the normalized efficiency $\eta/\eta_C = -J_w A_w / J_q A_q$, the steps that lead to Eq. (9) can be repeated one by one [59]. We thus find that η/η_C generically converges to 1 only if the quasi-static heat flux vanishes and both affinities go to zero with A_w vanishing faster than A_q , whereby η and η_C both approach zero. Close to this limit, the engine is subject to the power-efficiency trade-off relation

$$P \leq Z(\eta_C - \eta)^2 / \eta_C \quad (10)$$

and the optimal thermal gradient, for which it is saturated asymptotically, is given by $A_q^* = \sqrt{z A_w}$.

The bounds (9) and (10) ultimately arise from the fact that the Onsager symmetry (4) does not extend to the second-order coefficients L_{wq}^q and L_{qw}^q . Still, there are special situations, where $L_{wq}^q \simeq -L_{qw}^q$ [59]. Under this condition, the second term in the expansion (7) can be neglected and we are left with the trivial relation $\varepsilon =$

$(1 + L_{ww}A_w/L_{qw}A_q)\varepsilon_C$ [60]. The Carnot bound is then attained for any A_q in the limit $A_w \rightarrow 0$ with the power of the machine vanishing linearly. However, this behavior will typically occur only in fine-tuned systems. We stress that this restriction appears only when sub-leading terms in the expansions of the generalized fluxes are taken into account, cf. Eq. (13). It is therefore not captured by the established adiabatic-response theory, where both fluxes are assumed to be linear in affinities [51].

To unveil the geometric character of the bounds (9) and (10), we have to analyze the structure of Z . We assume that the machine is driven by periodic changes of the parameters $\lambda = \{\lambda^\mu\}$, which control the energy of the working system and its coupling to the baths. Once the system has settled to a periodic state, the work input and heat uptake from the reservoir per cycle are given by

$$W = - \int_0^\tau dt f_t^\mu \dot{\lambda}_t^\mu \quad \text{and} \quad Q = \int_0^\tau dt j_t, \quad (11)$$

where f_t^μ is the generalized force conjugate to the parameter λ^μ and j_t denotes the heat current from the reservoir into the system. If the driving is slow on the internal time-scale of the system and the difference between the inverse temperatures of reservoir and environment is small on its typical energy scale, these quantities can be expanded in the driving rates and the thermal gradient,

$$f_t^\mu = -\partial_\mu \mathcal{F}_{\lambda_t} - \mathcal{R}_{\lambda_t}^{\mu\nu} \beta_e \dot{\lambda}_t^\nu - \mathcal{R}_{\lambda_t}^{\mu q} A_q - \mathcal{R}_{\lambda_t}^{\mu qq} A_q^2, \quad (12a)$$

$$j_t = \mathcal{R}_{\lambda_t}^{q\mu} \beta_e \dot{\lambda}_t^\mu + \mathcal{R}_{\lambda_t}^{qq\mu} \beta_e \dot{\lambda}_t^\mu A_q. \quad (12b)$$

The free energy of the system \mathcal{F}_λ and the adiabatic-response coefficients \mathcal{R}_λ depend parametrically on the control vector λ and on β_e . Note that we include only the relevant second-order terms and assume that there are no heat-leaks, i.e. $j_t|_{\dot{\lambda}_t=0} = 0$.

Upon inserting the Eqs. (12) into Eq. (11) and comparing the result with the expansions of the fluxes,

$$J_w = L_{wx}A_x + L_{wq}^q A_q^2, \quad J_q = L_{qw}A_w + L_{qw}^q A_w A_q, \quad (13)$$

the off-diagonal coefficients can be expressed as line integrals in the space of control parameters,

$$\begin{bmatrix} L_{wq} & L_{qw} \\ L_{wq}^q & L_{qw}^q \end{bmatrix} = \oint_\gamma \begin{bmatrix} \mathcal{A}_\lambda^{\mu q} & \mathcal{A}_\lambda^{q\mu} \\ \mathcal{A}_\lambda^{\mu qq} & \mathcal{A}_\lambda^{qq\mu} \end{bmatrix} d\lambda^\mu. \quad (14)$$

Here, γ denotes the closed path that is mapped out by the driving protocols λ_t and the thermodynamic vector potentials are defined as

$$\begin{bmatrix} \mathcal{A}_\lambda^{\mu q} & \mathcal{A}_\lambda^{q\mu} \\ \mathcal{A}_\lambda^{\mu qq} & \mathcal{A}_\lambda^{qq\mu} \end{bmatrix} \equiv -\lambda^\nu \partial_\mu \begin{bmatrix} \mathcal{R}_\lambda^{\nu q} & \mathcal{R}_\lambda^{q\nu} \\ \mathcal{R}_\lambda^{\nu qq} & \mathcal{R}_\lambda^{qq\nu} \end{bmatrix} \quad (15)$$

The coefficient L_{ww} does not admit a geometric representation. It is, however, subject to the geometric bound

$$L_{ww} = \tau \int_0^\tau dt \mathcal{G}_{\lambda_t}^{\mu\nu} \dot{\lambda}_t^\mu \dot{\lambda}_t^\nu \geq \mathcal{L}^2 \quad \text{with} \quad \mathcal{L} \equiv \oint_\gamma \sqrt{\mathcal{G}_\lambda^{\mu\nu} d\lambda^\mu d\lambda^\nu} \quad (16)$$

being the thermodynamic length of the path γ . This notion is motivated by the fact that, owing to the second law, the coefficients $\mathcal{G}_\lambda^{\mu\nu} \equiv (\mathcal{R}_\lambda^{\mu\nu} + \mathcal{R}_\lambda^{\nu\mu})/2$ form a positive semi-definite matrix and can therefore be interpreted as a pseudo-Riemannian metric in the space of control parameters. The bound (16) can be derived by minimizing L_{ww} with respect to the parameterization of the path γ . The optimal parameterization ϕ_t , for which Eq. (16) becomes an equality, is implicitly determined by the condition

$$t = \frac{\tau}{\mathcal{L}} \int_0^{\phi_t} ds \sqrt{\mathcal{G}_{\lambda_s}^{\mu\nu} \dot{\lambda}_s^\mu \dot{\lambda}_s^\nu}. \quad (17)$$

The Eqs. (14) and (16) show that the figure of merit Z is subject to the bound $Z \leq \mathcal{Z} \equiv L_{qw}^3/4(L_{wq}^q + L_{qw}^q)\mathcal{L}^2$, where \mathcal{Z} depends only on geometric quantities. Thus, Eqs. (9) and (10) imply the geometric trade-off relations

$$J_q \leq \mathcal{Z}(\varepsilon_C - \varepsilon)^2/\varepsilon_C^2 \quad \text{and} \quad P \leq \mathcal{Z}(\eta_C - \eta)^2/\eta_C \quad (18)$$

for adiabatic refrigerators and heat engines. These bounds, which are our second main result, hold for any thermodynamically consistent dynamics that admits a well-defined adiabatic-response regime. Moreover, they are asymptotically saturated in the limit $A_w \rightarrow 0$ if the optimal parameterization ϕ_t is chosen for the control path γ and the thermal gradient is scales with the driving frequency as $A_q = \mp \sqrt{\hat{z} A_w}$ with $\hat{z} \equiv \mathcal{L}^2/(L_{wq}^q + L_{qw}^q)$.

Two-stroke cycles provide a general mechanism to fully suppress heat-leaks. Under this protocol, the working system is decoupled from the environment for the first part $\tau_1 < \tau$ of the cycle and decoupled from the reservoir during the second part $\tau - \tau_1$. As a result, no persistent heat current between reservoir and environment emerges and j_t and J_q vanish for $A_w \rightarrow 0$. The coefficients (14) then depend solely on equilibrium properties of the working system and the geometric figure of merit becomes

$$\mathcal{Z} = \frac{(\mathcal{S}_{\lambda_1} - \mathcal{S}_{\lambda_0})^3}{2\beta_e^3(\mathcal{C}_{\lambda_1} + \mathcal{C}_{\lambda_0})\mathcal{L}^2}, \quad (19)$$

where $\lambda_1 \equiv \lambda_{\tau_1}$ and \mathcal{S}_λ and \mathcal{C}_λ denote the equilibrium entropy and heat capacity of the working system at fixed control parameters and inverse temperature β_e [59]. Hence, the only quantity that still depends on the dynamics of the system is the thermodynamic length \mathcal{L} .

To illustrate the two-stroke mechanism, we consider a quantum refrigerator that consists of a qubit with Hamiltonian $H_\lambda = \hbar\Omega\lambda\sigma_z/2$, where Ω sets the energy scale [61, 62]. The state ρ_t of the system evolves according to the adiabatic Lindblad equation [63]

$$\partial_t \rho_t = -\frac{i}{\hbar} [H_{\lambda_t}, \rho_t] + D_{\lambda_t}^r \rho_t + D_{\lambda_t}^e \rho_t \quad (20)$$

with $D_{\lambda_t}^x \dots \equiv \Gamma \kappa_t^x \sum_{\alpha=\pm} n_{\lambda_t, \beta_x}^\alpha ([\sigma_\alpha \dots, \sigma_\alpha^\dagger] + [\sigma_\alpha, \dots \sigma_\alpha^\dagger])$ being dissipation super-operators that describe the influence of the reservoir and the environment ($x = r, e$).

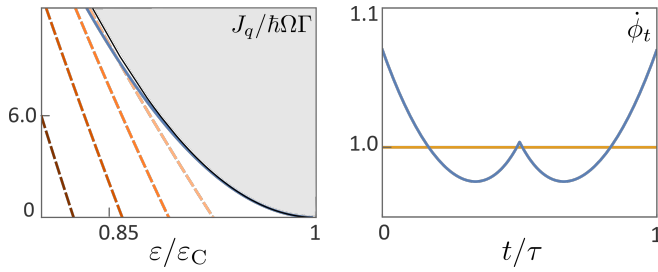


FIG. 1. Qubit refrigerator. The first plot shows the cooling power in units of $10^{-4}\hbar\Omega\Gamma$ as a function of the normalized COP, where τ is varied from $10^{-6}/\Gamma$ to $1/\Gamma$. Along the dashed lines, for which $1/\beta_r = 0.89, \dots, 0.95\hbar\Omega$ from left to right, the cooling power goes to zero at $\varepsilon/\varepsilon_C < 1$ in the limit $A_w \rightarrow 0$. The solid line, for which we set $A_q = -\sqrt{\tilde{z}}\overline{A}_w$, almost saturates the first bound (18). For all plots, we have set $1/\beta_e = \hbar\Omega$ and chosen the optimal parameterization of the control path ϕ_t , whose derivative is shown in the second plot.

Here, σ_z and σ_{\pm} are the usual Pauli matrices, the rate $\Gamma > 0$ sets the relaxation time scale of the system and $n_{\lambda, \beta_x}^+ \equiv 1/(e^{\beta_x \hbar\Omega\lambda} - 1)$ and $n_{\lambda, \beta_x}^- \equiv n_{\lambda, \beta_x}^+ + 1$ are thermal factors. For the control parameters $\lambda^1 \equiv \lambda$ and $\lambda^2 \equiv \kappa^r \equiv 1 - \kappa^e$, we choose the following protocols. During the first stroke, the system couples to the reservoir, i.e. $\kappa_t^r = 1$, and the level spacing λ_t decreases linearly from 2 to 1; in the second stroke, the system couples to the environment, i.e. $\kappa_t^r = 0$, and λ_t increases linearly from 1 to 2. For general adiabatic Lindblad dynamics, the generalized forces and the heat current are given by

$$f_t^\mu = -\text{tr}[\rho_t^r \partial_\mu H_{\lambda_t}] \quad \text{and} \quad j_t = \text{tr}[(D_{\lambda_t}^r \rho_t^r) H_{\lambda_t}], \quad (21)$$

where ρ_t^r is the periodic state of the system. These quantities can now be calculated perturbatively in the driving rates and the thermal gradient, which yields the thermodynamic length (16) and the figure of merit (19) for the qubit refrigerator [59]. To compare the performance of this device with the first trade-off relation (18), we calculate its COP and cooling power by solving the master equation (20) numerically. Fig. 1 shows that, in the quasi-static limit, ε remains indeed strictly smaller than ε_C for any fixed $A_q < 0$, while it approaches ε_C if A_q is optimized with respect to the cycle time; the bound (18) is asymptotically saturated if the optimal parameterization (17) is chosen for the control path.

This result shows that the sudden changes of the coupling parameters κ^r and κ^e are consistent with the adiabatic-response assumption. This conclusion holds in general for the weak-coupling regime, where the internal energy and the equilibrium state of the system do not depend on its interaction with the baths. Under this condition, the coupling parameters do not give rise to generalized forces and their time derivatives do not appear in the expansion (12a), see [59] for details. As a result, the coupling parameters do enter the diagonal kinetic coefficient (16) or the thermodynamic length. They

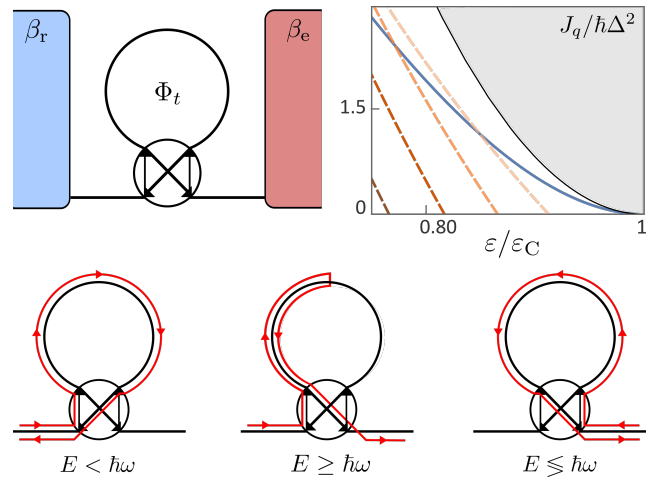


FIG. 2. Aharonov-Bohm refrigerator. A four-way beam splitter connects a mesoscopic ring and two ideal leads supporting a single transport channel. The left and the right lead are coupled to the cold reservoir and the environment, respectively. The linearly increasing magnetic flux Φ_t induces a constant electromagnetic force around the ring, which decelerates incoming carriers from the reservoir; carriers with energy $E \geq \hbar\omega$ pass through the ring and return to the reservoir; carriers with $E < \hbar\omega$ are reflected on the ring and transmitted to the environment. Incoming carriers from the environment are accelerated and return to the environment regardless of their energy. For $\omega \rightarrow 0$, no carriers are transmitted; hence, the quasi-static heat flux vanishes. The plot shows the cooling power of the device in units of $10^{-4}\hbar\Delta^2$ as a function of its normalized COP, where ω is varied from $10^{-7}\Delta$ to $10^{-2}\Delta$. Here, $2\pi/\Delta = 4\pi ml^2/\hbar$ is the typical dwell time, m denotes the carrier mass and l the circumference of the ring. The dashed lines correspond to $1/\beta_r = 0.90, \dots, 0.96\hbar\Delta$ from left to right. The blue line is obtained for $A_q = -\sqrt{\tilde{z}}\overline{A}_w$ and the gray area indicates the bound (18). For all plots, we have set $1/\beta_e = \hbar\Delta$ and $\mu = 1.05\hbar\Delta$ and used the optimal parameterization $\phi_t = t$.

rather affect only the off-diagonal coefficients (14), which, being geometric quantities, do not depend on the driving rates. The expansions (13) of the generalized fluxes are thus well-defined for the two-stroke protocol.

To show that the trade-off relations (18) are applicable also outside the two-stroke scheme, we now consider a mesoscopic refrigerator based on coherent transport. The system consists of a four-way beam-splitter and a mesoscopic ring subject to the time-dependent magnetic flux Φ_t , see Fig. 2 [64]. Its two control parameters can be identified with the real and the imaginary part of the Aharonov-Bohm phase that is picked by a particle when passing through the ring, i.e. $e^{iq\Phi/\hbar c} \equiv \lambda^1 + i\lambda^2$, where c is the speed of light and q the carrier charge. A linearly increasing flux, $\Phi_t \equiv \hbar c \omega t / q$, thus leads to the driving protocols $\lambda_t^1 = \cos[\omega t]$ and $\lambda_t^2 = \sin[\omega t]$, where $\omega = 2\pi/\tau$.

For coherent transport and effectively non-interacting carriers, the generalized forces and the heat current ad-

mit the general expressions [39, 65, 66]

$$f_t^\mu = - \int_0^\infty dE \sum_{x=r,e} \langle \psi_{E,t}^x | \partial_\mu H_{\lambda_t} | \psi_{E,t}^x \rangle g_E^x \quad \text{and} \quad (22a)$$

$$j_t = \int_0^\infty dE \sum_{x=r,e} \langle \psi_{E,t}^x | J_{\lambda_t} | \psi_{E,t}^x \rangle g_E^x. \quad (22b)$$

Here, H_λ and J_λ are the single-carrier Hamiltonian and heat current operator and $|\psi_{E,t}^x\rangle$ is the Floquet scattering state that describes a carrier with energy E , which enters the system either from the reservoir or the environment [66, 67]; $g_E^x \equiv 1/[1 + e^{\beta_x(E-\mu)}]$ is the Fermi function with chemical potential μ .

If the typical dwell time of carriers inside the system is short compared to τ , the Floquet-scattering states can be calculated perturbatively [39], which yields the figure of merit \mathcal{Z} for the Aharonov-Bohm refrigerator [59]. Since no carriers are transmitted for $\omega = 0$, the quasi-static heat flux vanishes and the first trade-off relation (18) applies. Fig. 2 shows how the cooling power and the COP of the Aharonov-Bohm refrigerator, which can be calculated exactly [59], compare to this bound in the slow-driving regime. As for the qubit-refrigerator, we find that ε does not reach ε_C for any fixed $A_q < 0$, while the trade-off relation (18) is asymptotically saturated in the quasi-static limit if A_q is optimized with respect A_w .

This outcome further underlines the universality of our main insights. First, generic adiabatic thermal machines cannot approach their Carnot limit when working between two baths with finite temperature difference. Second, close to this limit, the performance of such devices is not captured by standard adiabatic-response theory, which treats both temperature gradient and driving rates as first-order perturbations. Instead, second-order terms describing corrections to the finite-rate heat current and the non-isothermal work play an essential role. Taking these corrections into account leads to the geometric trade-off relations (18), which imply that power decays quadratically rather than linear at the Carnot bound. These results follow only from system-independent arguments and the Onsager symmetry (4). It now remains to future research to explore how breaking this symmetry alters the performance of adiabatic thermal machines.

Acknowledgments: The authors thank Thomas Venes for a careful proofreading of this manuscript. K.B. acknowledges support from the University of Nottingham through a Nottingham Research Fellowship and from UK Research and Innovation through a Future Leaders Fellowship (Grant Reference: MR/S034714/1).

- bounds on efficiency for systems with broken time-reversal symmetry, *Phys. Rev. Lett.* **106**, 230602 (2011).
- [3] K. Brandner, K. Saito, and U. Seifert, Strong bounds on Onsager coefficients and efficiency for three-terminal thermoelectric transport in a magnetic field, *Phys. Rev. Lett.* **110**, 070603 (2013).
- [4] A. E. Allahverdyan, K. V. Hovhannisyanyan, A. V. Melkikh, and S. G. Gevorkian, Carnot cycle at finite power: Attainability of maximal efficiency, *Phys. Rev. Lett.* **111**, 050601 (2013).
- [5] V. Holubec and A. Ryabov, Maximum efficiency of low-dissipation heat engines at arbitrary power, *J. Stat. Mech.* **2016**, 73204 (2016).
- [6] M. Campisi and R. Fazio, The power of a critical heat engine, *Nat. Commun.* **7**, 11895 (2016).
- [7] M. Poletti and M. Esposito, Carnot efficiency at divergent power output, *EPL (Europhysics Letters)* **118**, 40003 (2017).
- [8] S. L. Lee and H. Park, Carnot efficiency is reachable in an irreversible process, *Sci. Rep.* **7**, 10725 (2017).
- [9] V. Holubec and A. Ryabov, Diverging, but negligible power at carnot efficiency: Theory and experiment, *Phys. Rev. E* **96**, 062107 (2017).
- [10] V. Holubec and A. Ryabov, Cycling tames power fluctuations near optimum efficiency, *Phys. Rev. Lett.* **121**, 120601 (2018).
- [11] T. Koyuk, U. Seifert, and P. Pietzonka, A generalization of the thermodynamic uncertainty relation to periodically driven systems, *J. Phys. A: Math. Theor.* **52**, 02LT02 (2019).
- [12] K. Miura, Y. Izumida, and K. Okuda, Compatibility of Carnot efficiency with finite power in an underdamped brownian Carnot cycle in small temperature-difference regime, *Phys. Rev. E* **103**, 042125 (2021).
- [13] K. Brandner and U. Seifert, Bound on thermoelectric power in a magnetic field within linear response, *Phys. Rev. E* **91**, 012121 (2015).
- [14] K. Brandner, K. Saito, and U. Seifert, Thermodynamics of micro- and nano-systems driven by periodic temperature variations, *Phys. Rev. X* **5**, 031019 (2015).
- [15] K. Proesmans and C. Van den Broeck, Onsager coefficients in periodically driven systems, *Phys. Rev. Lett.* **115**, 090601 (2015).
- [16] K. Proesmans, B. Cleuren, and C. Van den Broeck, Power-efficiency-dissipation relations in linear thermodynamics, *Phys. Rev. Lett.* **116**, 220601 (2016).
- [17] K. Brandner and U. Seifert, Periodic thermodynamics of open quantum systems, *Phys. Rev. E* **93**, 062134 (2016).
- [18] N. Shiraishi, K. Saito, and H. Tasaki, Universal trade-off relation between power and efficiency for heat engines, *Phys. Rev. Lett.* **117**, 190601 (2016).
- [19] P. Pietzonka and U. Seifert, Universal trade-off between power, efficiency, and constancy in steady-state heat engines, *Phys. Rev. Lett.* **120**, 190602 (2018).
- [20] T. Koyuk and U. Seifert, Operationally accessible bounds on fluctuations and entropy production in periodically driven systems, *Phys. Rev. Lett.* **122**, 230601 (2019).
- [21] T. Kamijima, S. Otsubo, Y. Ashida, and T. Sagawa, Higher-order efficiency bound and its application to non-linear nanothermoelectrics, *Phys. Rev. E* **104**, 044115 (2021).
- [22] N. Shiraishi and K. Saito, Fundamental relation between entropy production and heat current, *J. Stat. Phys.* **174**, 433 (2019).

- [1] H. B. Callen, *Thermodynamics and an Introduction to Thermostatistics*, 2nd ed. (John Wiley & Sons, New York, 1985).
- [2] G. Benenti, K. Saito, and G. Casati, Thermodynamic

- [23] P. Menczel, C. Flindt, and K. Brandner, Quantum jump approach to microscopic heat engines, *Phys. Rev. Research* **2**, 033449 (2020).
- [24] R. S. Whitney, Most efficient quantum thermoelectric at finite power output, *Phys. Rev. Lett.* **112**, 130601 (2014).
- [25] R. S. Whitney, Finding the quantum thermoelectric with maximal efficiency and minimal entropy production at given power output, *Phys. Rev. B* **91**, 115425 (2015).
- [26] E. Potanina, C. Flindt, M. Moskalets, and K. Brandner, Thermodynamic bounds on coherent transport in periodically driven conductors, *Phys. Rev. X* **11**, 021013 (2021).
- [27] K. Miura, Y. Izumida, and K. Okuda, Achieving Carnot efficiency in finite-power brownian Carnot cycle with arbitrary temperature difference (2021), [arXiv:2112.02276](https://arxiv.org/abs/2112.02276) [[cond-mat.stat-mech](https://arxiv.org/abs/2112.02276)].
- [28] F. Weinhold, Metric geometry of equilibrium thermodynamics, *J. Chem. Phys.* **63**, 2479 (1975).
- [29] R. Gilmore, Length and curvature in the geometry of thermodynamics, *Phys. Rev. A* **30**, 1994 (1984).
- [30] B. Andresen, R. S. Berry, R. Gilmore, E. Ihrig, and P. Salamon, Thermodynamic geometry and the metrics of Weinhold and Gilmore, *Phys. Rev. A* **37**, 845 (1988).
- [31] G. Ruppeiner, Riemannian geometry in thermodynamic fluctuation theory, *Rev. Mod. Phys.* **67**, 605 (1995).
- [32] G. E. Crooks, Measuring thermodynamic length, *Phys. Rev. Lett.* **99**, 100602 (2007).
- [33] D. A. Sivak and G. E. Crooks, Thermodynamic metrics and optimal paths, *Phys. Rev. Lett.* **108**, 190602 (2012).
- [34] P. R. Zulkowski, D. A. Sivak, G. E. Crooks, and M. R. DeWeese, Geometry of thermodynamic control, *Phys. Rev. E* **86**, 041148 (2012).
- [35] B. B. Machta, Dissipation bound for thermodynamic control, *Phys. Rev. Lett.* **115**, 260603 (2015).
- [36] P. W. Brouwer, Scattering approach to parametric pumping, *Phys. Rev. B* **58**, R10135 (1998).
- [37] M. Scandi and M. Perarnau-Llobet, Thermodynamic length in open quantum systems, *Quantum* **3**, 197 (2019).
- [38] H. J. D. Miller, M. Scandi, J. Anders, and M. Perarnau-Llobet, Work fluctuations in slow processes: Quantum signatures and optimal control, *Phys. Rev. Lett.* **123**, 230603 (2019).
- [39] M. Thomas, T. Karzig, S. V. Kusminskiy, G. Zaránd, and F. von Oppen, Scattering theory of adiabatic reaction forces due to out-of-equilibrium quantum environments, *Phys. Rev. B* **86**, 195419 (2012).
- [40] M. F. Ludovico, F. Battista, F. von Oppen, and L. Arrachea, Adiabatic response and quantum thermoelectrics for ac-driven quantum systems, *Phys. Rev. B* **93**, 075136 (2016).
- [41] V. Cavina, A. Mari, and V. Giovannetti, Slow dynamics and thermodynamics of open quantum systems, *Phys. Rev. Lett.* **119**, 050601 (2017).
- [42] R. Bustos-Marún, G. Refael, and F. von Oppen, Adiabatic quantum motors, *Phys. Rev. Lett.* **111**, 060802 (2013).
- [43] Y. Izumida, Hierarchical onsager symmetries in adiabatically driven linear irreversible heat engines, *Phys. Rev. E* **103**, L050101 (2021).
- [44] Y. Hino and H. Hayakawa, Geometrical formulation of adiabatic pumping as a heat engine, *Phys. Rev. Research* **3**, 013187 (2021).
- [45] K. Brandner and K. Saito, Thermodynamic geometry of microscopic heat engines, *Phys. Rev. Lett.* **124**, 040602 (2020).
- [46] H. J. D. Miller and M. Mehboudi, Geometry of work fluctuations versus efficiency in microscopic thermal machines, *Phys. Rev. Lett.* **125**, 260602 (2020).
- [47] H. J. D. Miller, M. H. Mohammady, M. Perarnau-Llobet, and G. Guarnieri, Thermodynamic uncertainty relation in slowly driven quantum heat engines, *Phys. Rev. Lett.* **126**, 210603 (2021).
- [48] A. G. Frim and M. R. DeWeese, A geometric bound on the efficiency of irreversible thermodynamic cycles (2021), [arXiv:2112.10797](https://arxiv.org/abs/2112.10797) [[cond-mat.stat-mech](https://arxiv.org/abs/2112.10797)].
- [49] H. Hayakawa, V. M. M. Paasonen, and R. Yoshii, Geometrical quantum chemical engine (2021), [arXiv:2112.12370](https://arxiv.org/abs/2112.12370) [[cond-mat.stat-mech](https://arxiv.org/abs/2112.12370)].
- [50] J. Lu, Z. Wang, J. Peng, C. Wang, J.-H. Jiang, and J. Ren, Geometric thermodynamic uncertainty relation in periodically driven thermoelectric heat engine (2022), [arXiv:2201.02477](https://arxiv.org/abs/2201.02477) [[cond-mat.mes-hall](https://arxiv.org/abs/2201.02477)].
- [51] B. Bhandari, P. T. Alonso, F. Taddei, F. von Oppen, R. Fazio, and L. Arrachea, Geometric properties of adiabatic quantum thermal machines, *Phys. Rev. B* **102**, 155407 (2020).
- [52] N. Pancotti, M. Scandi, M. T. Mitchison, and M. Perarnau-Llobet, Speed-ups to isothermality: Enhanced quantum thermal machines through control of the system-bath coupling, *Phys. Rev. X* **10**, 031015 (2020).
- [53] P. Abiuso, H. J. D. Miller, M. Perarnau-Llobet, and M. Scandi, Geometric optimisation of quantum thermodynamic processes, *Entropy* **22**, 110606 (2020).
- [54] R. Xu, A numerical method to find the optimal thermodynamic cycle in microscopic heat engine, *J. Stat. Phys.* **184** (2021).
- [55] P. T. Alonso, P. Abiuso, M. Perarnau-Llobet, and L. Arrachea, Geometric optimization of non-equilibrium adiabatic thermal machines and implementation in a qubit system (2021), [arXiv:2109.12648](https://arxiv.org/abs/2109.12648) [[quant-ph](https://arxiv.org/abs/2109.12648)].
- [56] G. Watanabe and Y. Minami, Finite-time thermodynamics of fluctuations in microscopic heat engines, *Phys. Rev. Research* **4**, L012008 (2022).
- [57] U. Seifert, Stochastic thermodynamics, fluctuation theorems and molecular machines, *Rep. Prog. Phys.* **75**, 126001 (2012).
- [58] To see that $Z, z \geq 0$, first notice that the refrigerator condition $J_q \geq 0$ requires that $L_{qw} \geq 0$, since $J_q = L_{qw}A_w$ in leading order in the affinities and $A_w \geq 0$. Second, observe that the rate of entropy production is given by $\sigma = L_{ww}A_w^2 + (L_{qw}^q + L_{wq}^q)A_wA_q^2$ at leading order. The second law $\sigma \geq 0$ thus requires $L_{qw}^q + L_{wq}^q \geq 0$.
- [59] See the Supplemental Material at [\[URL\]](https://arxiv.org/abs/2112.02276) for a derivation of the bound (10), general adiabatic-response coefficients for Lindblad dynamics and coherent transport and details on the qubit and Aharonov-Bohm refrigerators.
- [60] For heat engines, the symmetry $L_{wq} \simeq -L_{qw}$ leads to the analogous relation $\eta = (1 - L_{ww}A_w/L_{qw}A_q)\eta_C$.
- [61] A. O. Niskanen, Y. Nakamura, and J. P. Pekola, Information entropic superconducting microcooler, *Phys. Rev. B* **76**, 174523 (2007).
- [62] B. Karimi and J. P. Pekola, Otto refrigerator based on a superconducting qubit: Classical and quantum performance, *Phys. Rev. B* **94**, 184503 (2016).
- [63] T. Albash, S. Boixo, D. A. Lidar, and P. Zanardi, Quantum adiabatic markovian master equations, *New J. Phys.* **14**, 123016 (2012).
- [64] J. E. Avron, A. Elgart, G. M. Graf, and L. Sadun, Optimal quantum pumps, *Phys. Rev. Lett.* **87**, 236601 (2001).

- [65] N. Bode, S. V. Kusminskiy, and F. Egger, R. and von Oppen, Current-induced forces in mesoscopic systems: A scattering-matrix approach, *Beilstein J. Nanotechnol.* **3**, 144 (2012).
- [66] K. Brandner, Coherent transport in periodically driven mesoscopic conductors: From scattering amplitudes to quantum thermodynamics, *Z. Naturforsch. A* **75**, 483 (2020).
- [67] M. Moskalets and M. Büttiker, Floquet scattering theory of quantum pumps, *Phys. Rev. B* **66**, 205320 (2002).

Geometric Bounds on the Power of Adiabatic Thermal Machines - Supplemental Material -

Joshua Eglinton and Kay Brandner

School of Physics and Astronomy, University of Nottingham, Nottingham NG7 2RD, United Kingdom

Centre for the Mathematics and Theoretical Physics of Quantum Non-equilibrium Systems,

University of Nottingham, Nottingham NG7 2RD, United Kingdom

(Dated: February 18, 2022)

I. PREAMBLE

This supplemental material consists of three parts: In Sec. II, we derive the power-efficiency trade-off relation for adiabatic heat engines that was discussed in the main text. In Sec. III, we provide general expressions for the kinetic coefficients of two-stroke cycles along with a detailed discussion of the qubit refrigerator. In Sec. VI, we sketch the derivation of the kinetic coefficients for periodically driven coherent conductors and further discuss the Aharonov-Bohm refrigerator. All symbols are used with same definitions as in the main text. Equation numbers without additional indicator S refer to the main text.

II. POWER-EFFICIENCY TRADE-OFF RELATION FOR ADIABATIC HEAT ENGINES

The power-efficiency trade-off relation (10) can be derived by following the same steps that lead to the power-COP trade-off relation (9) in the main text. We first express the normalized efficiency as

$$\frac{\eta}{\eta_C} = -\frac{J_w A_w}{J_q A_q} = -\frac{K_{ww}(A_w/A_q) + K_{wq}}{K_{qq}(A_q/A_w) + K_{qw}}. \quad (\text{S1})$$

Assuming that the isothermal work does not vanish, i.e. $K_{ww} > 0$, this expression converges to 1 in the quasi-static limit $A_w \rightarrow 0$ if $K_{qq} = 0$; this observation follows directly from the Onsager symmetry (4). To determine, how the power of the engine decays in this limit, we insert the expansions (6) for the coefficients K_{wq} and K_{qw} into Eq. (S1). Keeping only leading and first sub-leading contributions yields

$$\frac{\eta}{\eta_C} = 1 - \frac{L_{qw}^q + L_{wq}^w}{L_{qw}} A_q - \frac{L_{ww}}{L_{qw}} \frac{A_w}{A_q}. \quad (\text{S2})$$

Maximising this expression with respect to A_q returns the results

$$\eta/\eta_C \leq 1 - \sqrt{L_{qw} A_w / Z} \quad \text{and} \quad A_q^* = \sqrt{z A_w}, \quad (\text{S3})$$

for the upper bound on the normalized efficiency and the optimum of A_q . Note that the condition $J_w < 0$ requires $L_{wq} < 0$ and thus $L_{qw} > 0$. Finally, we observe that the power output of a heat engine, $P = -W/\tau = -A_w J_w / \beta_e$, reduces to $P = -L_{wq} A_w A_q / \beta_e$ in leading order in the

affinities. Thus, we can eliminate A_w in favor of P in the bound (S1), which leaves us with the result

$$P \leq Z(\eta_C - \eta)^2 / \eta_C. \quad (\text{S4})$$

Here, we have used that $L_{wq} = -L_{qw}$ and $\eta_C = A_q / \beta_e$.

III. TWO-STROKE CYCLES

In the following, we derive microscopic expressions for the adiabatic-response coefficients describing general two-stroke cycles and calculate these coefficients explicitly for the qubit-refrigerator discussed in the main text.

A. Kinetic Coefficients

We consider a thermal machine, whose working system is described by the Hamiltonian H_{λ} . The system is driven into a periodic state ρ_t^{τ} through cyclic variations of the control parameters $\lambda = \{\lambda^{\mu}\}$. During the first stroke of the cycle, where $0 \leq t < \tau_1$, the system is coupled to a reservoir with inverse temperature β_r ; during the second stroke, where $\tau_1 \leq t < \tau$, it couples to an environment with inverse temperature β_e . The energy balance of the machine is described by the first law

$$\dot{E}_t = -f_t^{\mu} \dot{\lambda}_t^{\mu} + j_t \quad (\text{S5})$$

where $E_t = \text{tr}[\rho_t^{\tau} H_{\lambda_t}]$ denotes the internal energy of the working system. The generalized forces and the rate of heat uptake are given by

$$f_t^{\mu} = -\text{tr}[\rho_t^{\tau} \partial_{\mu} H_{\lambda_t}] \quad \text{and} \quad j_t = \text{tr}[\dot{\rho}_t^{\tau} H_{\lambda_t}]. \quad (\text{S6})$$

Hence, the applied work in the first and the second stroke can be expressed as

$$W_1 = -\int_0^{\tau_1} dt f_t^{\mu} \dot{\lambda}_t^{\mu} \quad \text{and} \quad W_2 = -\int_{\tau_1}^{\tau} dt f_t^{\mu} \dot{\lambda}_t^{\mu}. \quad (\text{S7})$$

In the adiabatic-response regime, the generalized forces can be expanded as

$$f_t^{\mu} = -\partial_{\mu} \mathcal{F}_{\lambda_t}^x - \beta_e \mathcal{R}_{\lambda_t}^{\mu\nu} \dot{\lambda}_t^{\nu}, \quad (\text{S8})$$

where \mathcal{F}_{λ}^x denotes the equilibrium free energy of the system at the inverse temperature β_x with $x = r$ during the first stroke and $x = e$ during the second stroke. The

adiabatic-response coefficient $\mathcal{R}_\lambda^{\mu\nu}$ depend only on β_e , since we neglect cross terms between the driving rates and the thermal gradient $A_q = \beta_e - \beta_r$. Note that Eq. (S8) follows directly from the definition of the generalized forces (S6) and the assumption that the system follows its Gibbs state $\varrho_\lambda^x = \exp[-\beta_x(H_\lambda - \mathcal{F}_\lambda^x)]$ in the quasi-static limit.

Using Eqs. (S7) and (S8) the applied work in the first and the second stroke can now be expressed as

$$W_1 = \mathcal{F}_{\lambda_1}^r - \mathcal{F}_{\lambda_0}^r + \beta_e \int_0^{\tau_1} dt \mathcal{R}_{\lambda_t}^{\mu\nu} \dot{\lambda}_t^\mu \dot{\lambda}_t^\nu, \quad (\text{S9a})$$

$$W_2 = \mathcal{F}_{\lambda_0}^e - \mathcal{F}_{\lambda_1}^e + \beta_e \int_{\tau_1}^\tau dt \mathcal{R}_{\lambda_t}^{\mu\nu} \dot{\lambda}_t^\mu \dot{\lambda}_t^\nu, \quad (\text{S9b})$$

where we have used the shorthand notation $\lambda_1 = \lambda_{\tau_1}$. With the help of the thermodynamic standard relations $\beta^2 \partial_\beta \mathcal{F}_\lambda = \mathcal{S}_\lambda$ and $-\beta^3 \partial_\beta^2 \mathcal{F}_\lambda = 2\mathcal{S}_\lambda + \mathcal{C}_\lambda$, where \mathcal{S}_λ and \mathcal{C}_λ denote the entropy and heat capacity of the system, the free energies at the reservoir temperature in Eq. (S9a) can be expanded to second order in A_q . The applied work per cycle, $W = W_1 + W_2$, thus becomes

$$W = -\frac{A_q}{\beta_e^2} (\mathcal{S}_{\lambda_1} - \mathcal{S}_{\lambda_0}) - \frac{A_q^2}{\beta_e^3} (\mathcal{S}_{\lambda_1} - \mathcal{S}_{\lambda_0}) - \frac{A_q^2}{2\beta_e^3} (\mathcal{C}_{\lambda_1} - \mathcal{C}_{\lambda_0}) + \beta_e \int_0^\tau dt \mathcal{G}_{\lambda_t}^{\mu\nu} \dot{\lambda}_t^\mu \dot{\lambda}_t^\nu, \quad (\text{S10})$$

with $\mathcal{G}_\lambda^{\mu\nu} = (\mathcal{R}_\lambda^{\mu\nu} + \mathcal{R}_\lambda^{\nu\mu})/2$ and \mathcal{S}_λ and \mathcal{C}_λ being taken at the temperature of the environment. Comparing Eq. (S10) with the adiabatic-response expansion (13) of the generalized flux $J_w = W$ yields the kinetic coefficients

$$L_{ww} = \tau \int_0^\tau dt \mathcal{G}_{\lambda_t}^{\mu\nu} \dot{\lambda}_t^\mu \dot{\lambda}_t^\nu \quad (\text{S11a})$$

$$L_{wq} = -\frac{1}{\beta_e^2} (\mathcal{S}_{\lambda_1} - \mathcal{S}_{\lambda_0}), \quad (\text{S11b})$$

$$L_{wq}^q = -\frac{1}{\beta_e^3} (\mathcal{S}_{\lambda_1} - \mathcal{S}_{\lambda_0}) - \frac{1}{2\beta_e^3} (\mathcal{C}_{\lambda_1} - \mathcal{C}_{\lambda_0}). \quad (\text{S11c})$$

To calculate the heat uptake from the reservoir, we first observe that, in the quasi-static limit, the state of the system changes instantly from $\rho_{\lambda_0}^e$ to $\rho_{\lambda_0}^r$ at $t = 0$ and from $\rho_{\lambda_1}^r$ to $\rho_{\lambda_1}^e$ at $t = \tau_1$. These sudden changes occur due to the relaxation dynamics of the system being effectively infinitely fast on the observational time scale. They lead to delta-spikes in the heat current j_t , which correspond to heat leaks from the system to the reservoir at $t = 0$ and from the system to the environment at $t = \tau_1$. Hence, the total heat uptake from the reservoir is given by

$$Q = \lim_{\epsilon \rightarrow 0} \int_{0-\epsilon}^{\tau_1-\epsilon} dt j_t = \lim_{\epsilon \rightarrow 0} (E_{\tau_1-\epsilon} - E_{0-\epsilon}) - W_1, \quad (\text{S12})$$

where we have used the first law (S5). Note that this effect does not play a role for the extracted work, since, assuming that the control protocols λ_t^μ are continuous in t , the thermodynamic forces f_t^μ remain bounded functions of t in the quasi-static limit. Hence, no work is done during the switching between reservoir and environment.

Upon neglecting finite-rate corrections, the heat uptake (S12) becomes

$$Q = \mathcal{E}_{\lambda_1}^r - \mathcal{E}_{\lambda_0}^e - \mathcal{F}_{\lambda_1}^r + \mathcal{F}_{\lambda_0}^r, \quad (\text{S13})$$

where \mathcal{E}_λ^x denotes the equilibrium internal energy of the system at the inverse temperature β_x . Expanding this expression to first order in A_q yields

$$Q = \frac{1}{\beta_e} (\mathcal{S}_{\lambda_1} - \mathcal{S}_{\lambda_0}) + \frac{A_q}{\beta_e^2} (\mathcal{S}_{\lambda_1} - \mathcal{S}_{\lambda_0}) + \frac{A_q}{\beta_e^2} \mathcal{C}_{\lambda_1}. \quad (\text{S14})$$

Upon recalling the definition of the heat flux, $J_q = Q/\tau$, and comparing Eq. (S14) with the expansion (13), we can now identify the remaining kinetic coefficients as

$$L_{qw} = \frac{1}{\beta_e^2} (\mathcal{S}_{\lambda_1} - \mathcal{S}_{\lambda_0}), \quad (\text{S15a})$$

$$L_{qw}^q = \frac{1}{\beta_e^3} (\mathcal{S}_{\lambda_1} - \mathcal{S}_{\lambda_0}) + \frac{\mathcal{C}_{\lambda_1}}{\beta_e^3}. \quad (\text{S15b})$$

Thus, the geometric figure of merit \mathcal{Z} becomes

$$\mathcal{Z} = \frac{L_{qw}^3}{4(L_{qw}^q + L_{wq}^q)\mathcal{L}^2} = \frac{(\mathcal{S}_{\lambda_1} - \mathcal{S}_{\lambda_0})^3}{2\beta_e^3 (\mathcal{C}_{\lambda_1} + \mathcal{C}_{\lambda_0}) \mathcal{L}^2}, \quad (\text{S16})$$

which is the expression given in Eq. (19) of the main text.

B. Qubit refrigerator

1. Kinetic coefficients

We consider the qubit-refrigerator described in the main text. The system is controlled by two parameters $\lambda^1 = \lambda$ and $\lambda^2 \equiv \kappa^r \equiv 1 - \kappa^e$, which determines the level splitting and the coupling of the qubit to the reservoir and environment, respectively. The qubit Hamiltonian is

$$H_\lambda = \frac{\hbar\Omega}{2} \lambda \sigma_z, \quad (\text{S17})$$

where σ_z is the usual Pauli matrix and $\hbar\Omega$ sets the energy scale. The device is driven through a two-stroke cycle as described in the previous section. In the first stroke, λ is varied linearly from 2 to 1 while $\kappa^r = 1$ such that the system is coupled to the reservoir at inverse temperature β_r . In the second stroke, λ is linearly returned to its initial value with $\kappa^r = 0$, i.e. the qubit exchanges heat with the environment, whose inverse temperature is β_e .

For slow driving, the dynamics of the system can be described in terms of the adiabatic master equation [1],

$$\partial_t \rho_t = -\frac{i}{\hbar} [H_{\lambda_t}, \rho_t] + \text{D}_{\lambda_t}^r \rho_t + \text{D}_{\lambda_t}^e \rho_t, \quad (\text{S18})$$

where the dissipation super-operators are

$$\text{D}_\lambda^\alpha \cdots = \Gamma \kappa^x \sum_{\alpha=\pm} n_{\lambda, \beta_x}^\alpha ([\sigma_\alpha \cdots, \sigma_\alpha^\dagger] + [\sigma_\alpha, \cdots \sigma_\alpha^\dagger]). \quad (\text{S19})$$

Here, the rate $\Gamma > 0$ sets the relaxation time scale and $n_{\lambda, \beta_x}^+ \equiv 1/(e^{\beta_x \hbar \Omega \lambda} - 1)$ and $n_{\lambda, \beta_x}^- = 1 + n_{\lambda, \beta_x}^+$ are thermal factors; $\sigma_{\pm} = (\sigma_x \pm i\sigma_y)$ are the usual Pauli matrices. For fixed control parameters, the unique stationary solution of (S18) is given by the Gibbs state ϱ_{λ}^x .

The equilibrium free energy of the system at reads

$$\mathcal{F}_{\lambda} = -\frac{1}{\beta_e} \ln[2 \cosh[\theta \lambda]], \quad (\text{S20})$$

where $\theta = \hbar \Omega \beta_e / 2$. From this result, it is straightforward to calculate the equilibrium entropy and heat capacity,

$$\mathcal{S}_{\lambda} = \ln[2 \cosh[\theta \lambda]] - \theta \lambda \tanh[\theta \lambda], \quad (\text{S21a})$$

$$\mathcal{C}_{\lambda} = \frac{\theta^2 \lambda^2}{\cosh^2[\theta \lambda]}. \quad (\text{S21b})$$

Using Eqs. (S11) and (S15), we thus obtain the kinetic coefficients

$$L_{qw} = -L_{qw} = \frac{1}{\beta_e^2} \left(\ln[\cosh[\theta]] - \ln[\cosh[2\theta]] \right) - \frac{\theta}{\beta_e^2} \left(\tanh[2\theta] - 2 \tanh[\theta] \right), \quad (\text{S22a})$$

$$L_{wq}^q = \frac{\theta^2}{2\beta_e^3} \left(\frac{4}{\cosh^2[2\theta]} - \frac{1}{\cosh^2[\theta]} \right) - \frac{L_{qw}}{\beta_e}, \quad (\text{S22b})$$

$$L_{qw}^q = \frac{\theta^2}{\beta_e^3} \frac{1}{\cosh^2[\theta]} + \frac{L_{qw}}{\beta_e}. \quad (\text{S22c})$$

The coefficient L_{ww} must be found by perturbatively solving the master equation (S18). To this end, we make ansatz [2],

$$\rho_t \simeq \varrho_{\lambda}^e + R_{\lambda_t} \dot{\lambda}_t, \quad (\text{S23})$$

where R_{λ} is the first finite-rate correction to the state of the system. Substituting (S23) into Eq. (S18) and comparing coefficients gives

$$R_{\lambda} = L_{\lambda}^{-1} \partial_{\lambda} \varrho_{\lambda}, \quad (\text{S24})$$

where $L_{\lambda} \cdots = -\frac{i}{\hbar} [H_{\lambda}, \cdots] + D_{\lambda}^r \cdots + D_{\lambda}^e \cdots$, is the Lindblad generator for the qubit and L_{λ}^{-1} denotes its pseudo-inverse. Note that, since we are only interested in the coefficient L_{ww} , which describes the isothermal work contribution, we can set $\beta_r = \beta_e$. The generator L_{λ} does therefore not depend on the coupling parameter κ here.

Using the result (S24), we can evaluate the expression (S6) for the generalized force f_t , which gives the adiabatic-response coefficient

$$\mathcal{R}_{\lambda}^{11} = \mathcal{R}_{\lambda} = \frac{\hbar \Omega \theta}{4\beta_e \Gamma} \frac{\tanh[\theta \lambda_t]}{\cosh^2[\theta \lambda_t]}. \quad (\text{S25})$$

We thus have

$$L_{ww} = \frac{\hbar \Omega \theta \tau}{4\beta_e \Gamma} \int_0^{\tau} dt \frac{\tanh[\theta \lambda_t]}{\cosh^2[\theta \lambda_t]} \geq \mathcal{L}^2 \quad (\text{S26})$$

and the thermodynamic length is given by

$$\mathcal{L} = \frac{\hbar \Omega \theta \tau}{4\beta_e \Gamma} \oint_{\gamma} \sqrt{\tanh[\theta \lambda] / \cosh^2[\theta \lambda]} d\lambda \quad (\text{S27})$$

accordint to Eq. (16). The optimal speed function ϕ_t can now be found by numerically solving Eq. (17) with $\mathcal{G}_{\lambda}^{11} = \mathcal{R}_{\lambda}$.

2. Numerical Calculations

To obtain the exact dynamics of the qubit-refrigerator, we make the ansatz

$$\rho_t = \mathbb{I}/2 + \rho_t^z \sigma_z \quad (\text{S28})$$

for the state of the system, where \mathbb{I} denotes the identity matrix. Substituting this ansatz into Eq. (S18) yields differential equation

$$\partial_t \rho_t^z = -\Gamma \sum_{x=e,r} \kappa_t^x [2k_{\lambda_t, \beta_x}^+ \rho_t^z - k_{\lambda_t, \beta_x}^-], \quad (\text{S29})$$

with $k_{\lambda_t, \beta_x}^{\pm} = (n_{\lambda_t, \beta_x}^{\pm} \pm n_{\lambda_t, \beta_x})$. After specifying the control protocols λ_t as described before, we solve this equation numerically for ρ_t^z with periodic boundary conditions. Following Eq. (11), the applied work and heat uptake can then be found as

$$W = \hbar \Omega \int_0^{\tau} dt \rho_t^z \dot{\lambda}_t, \quad (\text{S30a})$$

$$J_q = -\frac{2\hbar \Omega \Gamma}{\tau} \int_0^{\tau_1} dt \frac{\rho_t^z \lambda_t}{\tanh[\theta_r \lambda_t]}, \quad (\text{S30b})$$

where $\theta_r = \hbar \Omega \beta_r / 2$. The cooling power and COP of the qubit-refrigerator are obtained by substituting the solution of (S29) into the expressions above for a range of cycle times τ .

IV. COHERENT TRANSPORT

In this section, we consider coherent conductors that are subject to slow periodic driving and coupled to two thermal baths with a small temperature difference, to which we refer as reservoir and environment. We first outline how the kinetic coefficients L_{xy} and L_{xy}^q can be obtained for such systems in general. In the second part, we focus on the Aharonov-Bohm refrigerator discussed at the end of the main text.

A. Kinetic Coefficients

We first recall the expressions for the generalized forces and the heat current from the reservoir into the system,

$$f_t^{\mu} = -\int_0^{\infty} dE \sum_{x=r,e} \langle \psi_{E,t}^x | \partial_{\mu} H_{\lambda_t} | \psi_{E,t}^x \rangle g_E^x \quad \text{and} \quad (\text{S31a})$$

$$j_t = \int_0^{\infty} dE \sum_{x=r,e} \langle \psi_{E,t}^x | J_{\lambda_t} | \psi_{E,t}^x \rangle g_E^x. \quad (\text{S31b})$$

Here, $g_E^x \equiv 1/[1 + e^{\beta x(E-\mu)}]$ denotes the Fermi function of either the reservoir ($x = r$) or the environment ($x = e$), where μ is the chemical potential. Furthermore,

$$H_\lambda = \frac{p^2}{2m} + V_\lambda(x), \quad (\text{S32a})$$

$$J_\lambda = -\frac{1}{4} \{ (H_\lambda - \mu), \{p, \delta[x - r_r]\} \} \quad (\text{S32b})$$

are the single-carrier Hamiltonian and the heat current operator, where x and p are the usual position and momentum operators, m is the carrier mass and V_λ is an externally tunable scattering potential, which vanishes outside a bounded scattering region. Curly brackets denote anti-commutators. The Floquet scattering states $|\psi_{E,t}^x\rangle$ describe a carrier with energy E that enters the conductor from the reservoir or the environment [3, 4]. These states are periodically dependent on t and satisfy the Floquet-Schrödinger equation

$$(H_{\lambda t} - i\hbar\partial_t)|\psi_{E,t}^x\rangle = E|\psi_{E,t}^x\rangle \quad (\text{S33})$$

with respect to the boundary conditions

$$\langle r_y|\psi_{E,t}^x\rangle = \delta_{xy}w_E^-[r_y] + S_{E,t}^{yx}w_E^+[r_y]. \quad (\text{S34})$$

Here, $w_\pm[r] = \xi_E e^{\pm ik_E r}$ are incoming (-) or outgoing (+) plane waves with wave number $k_E = [2mE/\hbar^2]^{\frac{1}{2}}$ and $\xi_E = [m/2\pi k_E \hbar^2]^{\frac{1}{2}}$ is a normalization factor. The spatial coordinate $r_x \geq 0$ parameterizes the lead that connects the scattering region with the bath x . For simplicity, we assume that the leads support only a single transport channel. Hence, they are effectively one-dimensional. Finally, the Floquet scattering amplitude $S_{E,t}^{yx}$, which is periodic in t , corresponds to the probability amplitude that a carrier with energy E is transmitted from the lead x to the lead y at the time t .

In the quasi-static limit, where the driving is infinitely slow compared to the dwell time of carriers inside the scattering region, the Floquet scattering states $|\psi_{E,t}^x\rangle$ reduce to the frozen scattering states $|\phi_{E,\lambda}^x\rangle$, which satisfy

$$H_\lambda|\phi_{E,\lambda}^x\rangle = E|\phi_{E,\lambda}^x\rangle \quad \text{and} \quad (\text{S35a})$$

$$\langle r_y|\phi_{E,\lambda}^x\rangle = \delta_{xy}w_E^-[r_y] + S_{E,\lambda}^{yx}w_E^+[r_y] \quad (\text{S35b})$$

with $S_{E,\lambda}^{yx}$ being the frozen scattering amplitudes. Finite-rate corrections to the Floquet scattering states can now be calculated by means of adiabatic perturbation theory [5, 6]. In first order, this approach yields

$$|\psi_{E,t}^x\rangle = |\phi_{E,\lambda_t}^x\rangle - i\hbar(G_{E,\lambda_t}^+)^2(\partial_\mu H_{\lambda_t})|\phi_{E,\lambda_t}^x\rangle\dot{\lambda}_t^\mu \quad (\text{S36})$$

with the retarded Greens function

$$G_{E,\lambda}^+ = \frac{1}{E - H_\lambda + i\epsilon}. \quad (\text{S37})$$

Upon inserting the approximation (S36) into the Eqs. (S31), the generalized forces f_t^μ and the heat current

j_t can be calculated to first order in the rates $\dot{\lambda}_t^\mu$. The fluxes J_x can then be obtained from Eqs. (1) and (11). Expanding in the thermal gradient A_q and comparing the result with the adiabatic-response relations

$$J_w = W = L_{ww}A_w + L_{wq}A_q + L_{wq}^q A_q^2, \quad (\text{S38})$$

$$J_q = Q/\tau = L_{qw}A_w + L_{qq}A_q + L_{qw}^q A_w A_q, \quad (\text{S39})$$

finally gives the kinetic coefficients L_{xy} and L_{xy}^q . This procedure can be carried out using standard manipulations of scattering theory. The final results are given by

$$L_{ww} = -\frac{\tau\hbar}{2} \int_0^\infty dE \frac{g'_E}{E - \mu} \sum_{x,y=e,r} \langle\langle |\dot{S}_{E,\lambda}^{xy}|^2 \rangle\rangle, \quad (\text{S40a})$$

$$L_{qq} = -\frac{1}{\tau\hbar} \int_0^\infty dE g'_E \langle\langle |S_{E,\lambda}^{re}|^2 \rangle\rangle, \quad (\text{S40b})$$

$$L_{wq} = \int_0^\infty dE g'_E \sum_{x=e,r} \text{Im}[\langle\langle \dot{S}_{E,\lambda}^{xr} S_{E,\lambda}^{rx*} \rangle\rangle], \quad (\text{S40c})$$

$$L_{qw} = -\int_0^\infty dE g'_E \sum_{x=e,r} \text{Im}[\langle\langle \dot{S}_{E,\lambda}^{rx} S_{E,\lambda}^{rx*} \rangle\rangle], \quad (\text{S40d})$$

$$L_{wq}^q = -\frac{1}{2} \int_0^\infty dE g''_E \sum_{x=e,r} \text{Im}[\langle\langle \dot{S}_{E,\lambda}^{xr} S_{E,\lambda}^{xr*} \rangle\rangle], \quad (\text{S40e})$$

$$L_{qw}^q = \frac{1}{\beta_e} \int_0^\infty dE (g'_E + \beta_e g''_E) \text{Im}[\langle\langle \dot{S}_{E,\lambda}^{rr} S_{E,\lambda}^{rr*} \rangle\rangle], \quad (\text{S40f})$$

where $\langle\langle \dots \rangle\rangle = \frac{1}{2\pi} \int_0^\tau dt \dots$ and we have introduced the abbreviations

$$g'_E = -g_E^e(1 - g_E^e)(E - \mu), \quad (\text{S41})$$

$$g''_E = g_E^e(1 - g_E^e)(1 - 2g_E^e)(E - \mu)^2. \quad (\text{S42})$$

Dots indicate total time derivatives. Notably, the expressions (S40) depend only on the frozen scattering amplitudes, which, unless time-reversal symmetry is broken, obey $S_{E,\lambda}^{xy} = S_{E,\lambda}^{yx}$. Hence, the coefficients L_{wq} and L_{qw} satisfy the Onsager symmetry (4). For details on the derivation of the Eqs. (S40), we refer the reader to the existing literature [3–7].

B. Aharonov-Bohm Refrigerator

1. Kinetic Coefficients

We now move on to the mesoscopic refrigerator shown in Fig. 2 of the main text. This model was originally introduced in Ref. [8] as an example for an ideal quantum pump. Its frozen scattering amplitudes are given by

$$S_{E,\lambda}^{re} = S_{E,\lambda}^{er} = 0, \quad S_{E,\lambda}^{rr} = \lambda^1 + i\lambda^2, \quad S_{E,\lambda}^{ee} = \lambda^1 - i\lambda^2, \quad (\text{S43})$$

where the two control parameters λ^1 and λ^2 correspond to the real and the imaginary part of the Aharonov-Bohm phase that is picked up by a carrier passing through the ring, i.e. $e^{iq\Phi/\hbar c} = \lambda^1 + i\lambda^2$. A linearly increasing magnetic

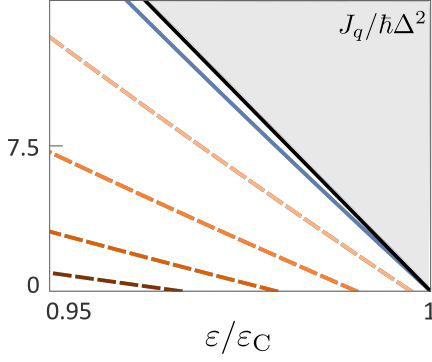


FIG. 1. Aharonov-Bohm refrigerator revisited. The cooling power in units $10^{-4}\hbar\Delta^2$ is plotted as a function of the normalised COP. For $A_w \rightarrow 0$, the linear bound (S50), shown by grey area, is approached asymptotically by the blue line, which corresponds to $\mu = 0$. By contrast, the dashed lines, for which we have set $\mu = 0.5\hbar\Delta, \dots, 2\hbar\Delta$ from top to bottom, do not reach the Carnot limit. For all curves, we have fixed the thermal gradient as $A_q = -\beta_e/24$ and scaled the driving frequency from $\omega = 10^{-6}\Delta$ to $\omega = 5 \times 10^{-3}\Delta$.

flux, $\Phi_t = \hbar\omega t/q$, thus leads to the driving protocols $\lambda_t^1 = \cos[\omega t]$ and $\lambda_t^2 = \sin[\omega t]$. For these protocols, it is straightforward to calculate the kinetic coefficients (S40). Specifically, we find

$$L_{ww} = \frac{2\pi\hbar\varphi}{\beta_e(1+\varphi)}, \quad (\text{S44a})$$

$$L_{qw} = -L_{wq} = -\frac{\mu\varphi}{\beta_e(1+\varphi)} + \frac{1}{\beta_e^2} \log[1+\varphi], \quad (\text{S44b})$$

$$L_{wq}^q = \frac{\mu\varphi(2+2\varphi-\beta_e\mu)}{2\beta_e^2(1+\varphi)^2} - \frac{1}{\beta_e^3} \log[1+\varphi], \quad (\text{S44c})$$

$$L_{qw}^q = -\frac{\mu\varphi(1+\varphi-\beta_e\mu)}{\beta_e^2(1+\varphi)^2} + \frac{1}{\beta_e^3} \log[1+\varphi] \quad (\text{S44d})$$

with $\varphi = e^{\beta_e\mu}$. Note that the coefficient L_{qq} is zero, since the quasi-static heat current vanishes as discussed in the main text. Furthermore, L_{ww} equals the square of the thermodynamic length \mathcal{L} , since the linear parameterization $\phi_t = t$ of the control path is optimal for this model.

2. Numerical Calculations

The exact Floquet scattering amplitudes for the Aharonov-Bohm device were calculated in App. D. of Ref. [7]. Using these results, the generalized fluxes can be written as

$$J_q = \frac{1}{2\pi\hbar} \int_0^\infty dE (E - \mu) ((g_E^r - g_{E+\hbar\omega}^r) + (g_{E+\hbar\omega}^r - g_E^e) T_E), \quad (\text{S45a})$$

$$J_w = - \int_0^\infty dE (g_{E+\hbar\omega}^r - g_E^e) \quad (\text{S45b})$$

with the transmission and reflection coefficients

$$T_E = \frac{|\hat{\mathbf{1}}^t \mathbb{A}_{E+\hbar\omega} \mathbb{A}_E^{-1} \mathbf{1}|^2}{|\mathbf{1}^t \mathbb{A}_{E+\hbar\omega} \mathbb{A}_E^{-1} \mathbf{1}|^2}, \quad R_E = \frac{4}{|\mathbf{1}^t \mathbb{A}_{E+\hbar\omega} \mathbb{A}_E^{-1} \mathbf{1}|^2}. \quad (\text{S46})$$

Here, $\mathbf{1} = (1, 1)^t$ and $\hat{\mathbf{1}}^t = (\hat{1}, -1)^t$ are vectors and the matrix \mathbb{A}_E is defined as

$$\mathbb{A}_E = \frac{1}{\xi_E} \begin{bmatrix} \text{Ai}_E & \text{Bi}_E \\ -i\text{Ai}'_E & -i\text{Bi}'_E \end{bmatrix} \quad (\text{S47})$$

with

$$\text{Xi}_E = \text{Xi}[(\omega/\Delta)^{-\frac{2}{3}}(-E/\hbar\Delta)], \quad (\text{S48a})$$

$$\text{Xi}'_E = (\omega/\Delta)^{\frac{1}{3}}(\hbar\Delta/E)^{\frac{1}{2}} \text{Xi}'[(\omega/\Delta)^{-\frac{2}{3}}(-E/\hbar\Delta)]. \quad (\text{S48b})$$

In these expressions, $\text{Xi} = \text{Ai}, \text{Bi}$ and $\text{Xi}' = \text{Ai}', \text{Bi}'$ denote the standard Airy functions and their derivatives. The parameter $2\pi/\Delta = 4\pi m l^2/\hbar^2$ corresponds to the typical dwell time of carriers inside the device. Hence, the adiabatic-response regime is defined by the condition $\omega/\Delta \ll 1$. We recall that ξ_E was defined below Eq. (S34) and that l is the circumference of the Aharonov-Bohm ring, see Fig. 2 of the main text. Upon evaluating the Eqs. (S45) numerically, we obtain the cooling power and efficiency of the Aharonov-Bohm refrigerator for arbitrary driving frequencies. These results provide us with a benchmark for the adiabatic-response theory.

3. Linear Trade-off Relations

The formulas (S40) for the kinetic coefficients of coherent conductors confirm that there is in general no obvious relation between the second-order coefficients L_{wq}^q and L_{qw}^q . However, there exist special situations, where $L_{wq}^q = -L_{qw}^q$. Under this condition, the first term in the expansion of the normalized COP, see Eq. (7), vanishes and we are left with the trivial relation

$$\varepsilon/\varepsilon_C = 1 + \frac{L_{ww}A_w}{L_{qw}A_q}. \quad (\text{S49})$$

This result indicates that the Carnot bound is attained in the quasi-static limit $A_w \rightarrow 0$ irrespective of A_q . Furthermore, since the cooling power is $J_q = L_{qw}A_w$ in leading order, we obtain the linear power-COP trade-off relation

$$J_q \leq Y(\varepsilon_C - \varepsilon)/\varepsilon_C, \quad (\text{S50})$$

where $Y = L_{qw}^2|A_q|/L_{ww} \geq 0$ [9].

We now return to the Aharonov-Bohm refrigerator. The sum of the second-order coefficients is

$$L_{wq}^q + L_{qw}^q = \frac{\mu^2 e^{\beta_e\mu}}{2\beta_e(1+e^{\beta_e\mu})^2}. \quad (\text{S51})$$

This quantity vanishes for $\mu \rightarrow 0$. Hence, in this limit, we expect that the device approaches its Carnot bound for any sufficiently small thermal gradient A_q as A_w goes to zero. Furthermore, its power output should decay linearly towards the Carnot limit. This behaviour is indeed confirmed by our numerical calculations, see Fig. 1.

-
- [1] T. Albash, S. Boixo, D. A. Lidar, and P. Zanardi, Quantum adiabatic markovian master equations, *New J. Phys.* **14**, 123016 (2012).
- [2] V. Cavina, A. Mari, and V. Giovannetti, Slow dynamics and thermodynamics of open quantum systems, *Phys. Rev. Lett.* **119**, 050601 (2017).
- [3] M. Moskalets and M. Büttiker, Floquet scattering theory of quantum pumps, *Phys. Rev. B* **66**, 205320 (2002).
- [4] K. Brandner, Coherent transport in periodically driven mesoscopic conductors: From scattering amplitudes to quantum thermodynamics, *Z. Naturforsch. A* **75**, 483 (2020).
- [5] M. Thomas, T. Karzig, S. V. Kusminskiy, G. Zaránd, and F. von Oppen, Scattering theory of adiabatic reaction forces due to out-of-equilibrium quantum environments, *Phys. Rev. B* **86**, 195419 (2012).
- [6] N. Bode, S. V. Kusminskiy, and F. Egger, R. and von Oppen, Current-induced forces in mesoscopic systems: A scattering-matrix approach, *Beilstein J. Nanotechnol.* **3**, 144 (2012).
- [7] E. Potanina, C. Flindt, M. Moskalets, and K. Brandner, Thermodynamic bounds on coherent transport in periodically driven conductors, *Phys. Rev. X* **11**, 021013 (2021).
- [8] J. E. Avron, A. Elgart, G. M. Graf, and L. Sadun, Optimal quantum pumps, *Phys. Rev. Lett.* **87**, 236601 (2001).
- [9] It is straightforward to derive the analogous trade-off relation for heat-engines, $P \leq Y(\eta_C - \eta)$.